On the Zigzag Form of Charged Domain Walls

Unusual domain walls have been found in ferrofluid patterns on thin film materials with low magnetization that is in or near the plane of the film. These walls carry a net magnetic charge and are characteristically kinked in a regular manner to form a zigzag. A simple account is given of the energetics of such walls whose form follows from a compromise between magnetostatic terms and the energy of anisotropy. It is argued that an array of closure domains at straight edges in these materials should have a boundary of similar character, and these too have been observed.

Introduction

Walls between magnetic domains are usually oriented so that the component of the magnetization M normal to the wall is continuous across the wall. Configurations can arise, however, in which the normal component of M is not the same on the two sides of a wall, and the wall is then magnetically charged. There is a cost of magnetostatic energy associated with the charge, and so such a wall is most likely to occur in materials with low values of saturation magnetization M_{c} or in very thin specimens. Jakubovics [1] has calculated the width of a charged domain wall for the case in which anisotropy confines M to the plane of the specimens. The energy is undetermined since the magnetostatic contribution depends on the location of the charge that compensates the charge on the wall. A somewhat surprising feature of Jakubovics' result is that for the parameters of interest in our work the charged wall is not significantly broader than an uncharged Néel wall.

Recent ferrofluid studies of magnetization distributions in sputtered Gd-Co films and in ion-implanted garnet films have shown a prevalence of sharply defined charged domain walls. These sharp walls characteristically have long uncurved sections but are only piecewise straight and kink with a consistent kink angle so as to form a zigzag across the sample. When these walls occur far from any feature, such as an unimplanted region in the garnet or the edge of the specimen, the amplitude of the zigzag is also fairly consistent. Figure 1 shows a ferrofluid picture of such a wall in an evaporated film of Gd-Co [2a]. Walls of

such character have been observed between head-on domains in Permalloy films [3, 4] by means of the Kerr magneto-optic effect and in magnetic films of Co and Co-Cr with use of Lorentz transmission microscopy [5], both techniques being without effect on the state of magnetization of the observed material. In this latter work it was noted that the entire region involving the kinked wall exhibited a nonuniform magnetization. A theoretical account [6] of the stability of such walls in thin films of Permalloy was based on the assumption that the magnetic charge associated with the wall was confined to the thin wall itself without significant spread of the charge into the triangular areas between adjacent segments of the wall. The vertex angle at the kinks was obtained from a minimization of energy made up of magnetostatic terms, anisotropy, and the wall energy per unit length. The zigzag amplitude of the structure was fixed by relating it to the coercive force of the material, although, as noted by Dressler and Judy [5], coercivity is not an intrinsic material property.

For the Gd-Co films and ion-implanted garnets the view is taken in this paper that the kinked, zigzag configuration is characteristic of the static magnetically charged wall, and that the shape results from a compromise between the magnetostatic energy associated with the charge on the wall and the anisotropy energy associated with deviations of M from an easy axis over a wide region. The geometrical characteristics of the zigzag are the vertex angle and the zigzag amplitude. The functional dependences of

Copyright 1979 by International Business Machines Corporation. Copying is permitted without payment of royalty provided that (1) each reproduction is done without alteration and (2) the *Journal* reference and IBM copyright notice are included on the first page. The title and abstract may be used without further permission in computer-based and other information-service systems. Permission to *republish* other excerpts should be obtained from the Editor.

these quantities on the intrinsic film properties—magnetization, anisotropy, and film thickness—are obtained in the following section.

Related to these zigzag walls in free space are the walls bounding closure domains along straight-edge boundaries between implanted and unimplanted regions in the garnet materials. These closure domains are discussed from the same point of view as presented in the discussion of zigzag walls in free space.

Gd-Co films

Evaporated films of Gd-Co are "amorphous" [2a, b] but are nonetheless endowed with an in-plane uniaxial anisotropy. The zigzag wall in Fig. 1 bounds two domains in a head-to-head arrangement. It should be noted that the full height of the zigzag is about $500~\mu m$, which is some four orders of magnitude larger than the film thickness or the width of a Néel wall. This disparity of scale occurs in other observations of the zigzag walls.

We consider a film with M confined to the plane of the film by a large anisotropy energy associated with any normal component of M as well as the magnetostatic energy. There is an easy axis of magnetization within the plane, as indicated in Fig. 2. Two oppositely oriented domains meet head-to-head along a horizontal boundary. If the film thickness is 2D, the magnetic charge per unit horizontal length is $4DM_{\rm s}$. If the wall should kink into a symmetrical zigzag with vertex angle 20, the length of the wall would be increased by a factor $(\sin \Theta)^{-1}$ while the linear charge density along the wall would be reduced by a factor $\sin \Theta$. One may imagine a contribution to the energy per unit length along the wall that is proportional to the square of the linear charge density (as may be inferred from Jakubovics' calculation), and so the kinked wall with its thinned-out charge would yield such an energy reduced by a factor $\sin \Theta$ as compared with the unkinked wall, thereby favoring the zigzag over the straight wall. There is, however, an inconsistency in such an assumed configuration. If the charge associated with the head-tohead abutting domains is assumed concentrated in the kinked wall, one can estimate the stray field within the horizontal band containing the wall. Comparing it with $2K/M_s$ in Gd-Co, for example, one finds that M deviates significantly from an easy direction throughout the wide band. That is, each segment of the wall has a rather extended tail, and there must exist a significant distributed charge. Thus, as compared with a straight horizontal wall, the magnetostatic energy is reduced by kinking, and further reduced by spread of the charge over a larger area. This spreading is accompanied by an increase in the anisotropy energy. We shall, in the following section, carry this idea to an extreme and estimate the contribu-

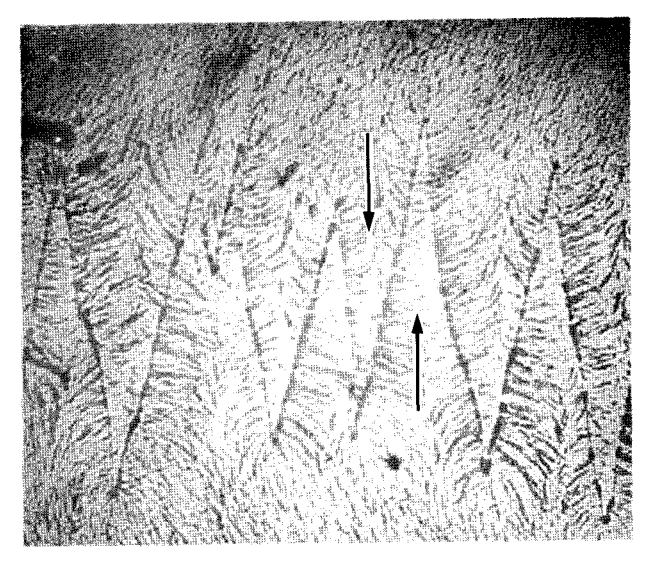


Figure 1 A ferrofluid pattern of a zigzag wall in an amorphous Gd-Co film with $2D=0.3~\mu m$, $4\pi M_s=0.32~T~(3200~Gs)$, and an in-plane uniaxial anisotropy constant $K=10^{-3}~\rm J/cm^3~(10^4~ergs/cm^3)$. The arrows indicate directions of magnetization in the domains.

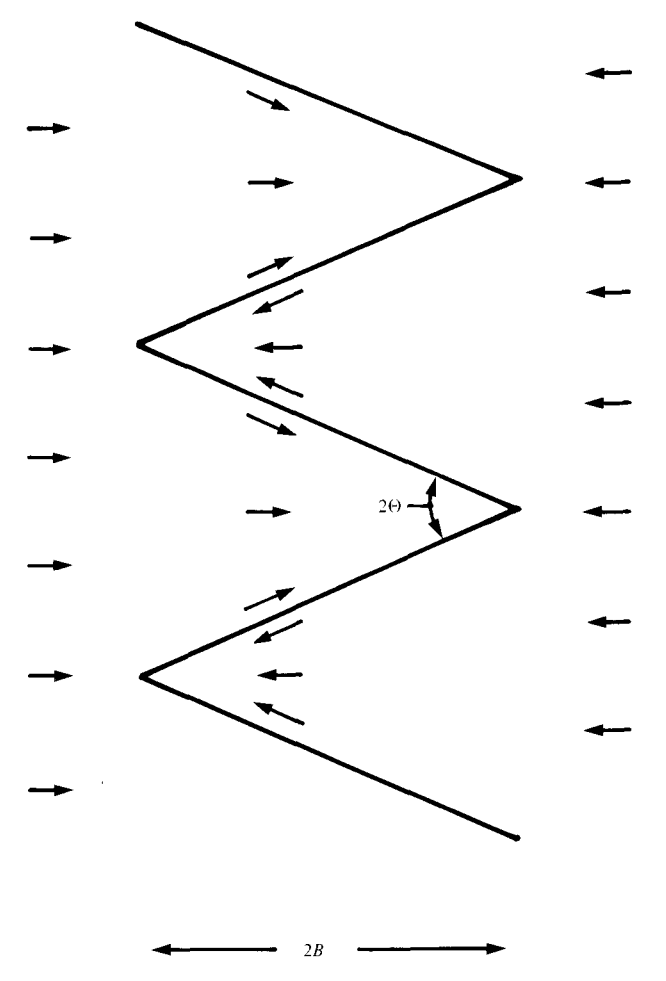


Figure 2 The magnetic configuration assumed for Gd-Co, corresponding to Fig. 1.

Table 1 Calculated and observed values of the vertex angle 2Θ and the bandwidth for charge distribution, 2B, in three Gd-Co films.

Sample	$4\pi M_{\rm s}$ (T)	2D (μm)	$(10^{-3} \text{ J/cm}^3 \text{ or} 10^4 \text{ ergs/cm}^3)$	Observed		Calculated	
				20 (degrees)	$\frac{2B}{(\mu m)}$	2⊖ (degrees)	2 <i>B</i> (μm)
a	0.32	0.30	1.0	23	500	10	2800
b	0.50	0.13	3.0	33	300-400	15	455
c	0.48	0.32	1.9	15-20	300-1000	6.5	9200

tions to the energy with the assumption that the charge is *uniformly* distributed over the entire band. Although this grossly exaggerates the diffuseness of the charge, it is found to give reasonable agreement with observations of the vertex angle and zigzag amplitude because major contributions to the energy are insensitive to details of the magnetization distribution.

Figure 2 exemplifies the type of configuration considered. The magnetic configuration is treated as if the charge were uniformly distributed along the y-axis over a band of width 2B. With M independent of z, the coordinate normal to the film, the volume charge density in the band is $M_{\rm s}/B$. With all the charge so distributed, the thin wall forming the zigzag is an uncharged $180^{\rm o}$ Néel wall. Three contributions to the energy must be taken into account: magnetostatic terms, anisotropy, and the energy of the residual Néel wall. Exchange does not enter explicitly because the scale of the structure is so large that the exchange contribution is negligible except as it is incorporated into the Néel wall energy.

We consider the zigzag band as traversing the center of a sample of width 2S, where S is very large (this turns out to be inconsequential). For a sample thickness 2D, in the limit of small D, the field due to the band of uniform charge is

$$H_x(x) = \frac{4M_sD}{B} \ln \frac{x+B}{x-B} \qquad |x| > B;$$

$$= \frac{4M_sD}{B} \ln \frac{B+x}{B-x} \qquad |x| < B. \tag{1}$$

The magnetostatic energy per unit horizontal length is

$$W_{\rm m} = \frac{D}{\Lambda} \int_{-s}^{s} dx \int_{0}^{\Lambda} dy \, H_{x}(x) M_{x}(x, y), \tag{2}$$

where $\Lambda = 4B \tan \Theta$ is the period of the zigzag. The angle between H and M is very nearly 0 or π , differing from one of these values by at most Θ . Up to terms of order $M_s^2 D^2 \Theta^2$, one obtains for the magnetostatic energy

$$W_{\rm m} = 8M_s^2 D^2 \left(3 - 2 \ln \frac{2B}{s} \right). \tag{3}$$

(For the materials to be considered here, the coefficient of

the Θ^2 term in the magnetostatic energy is only a percent or so of that in the anisotropy energy for which the entire contribution is proportional to Θ^2 .)

For the assumed configuration the anisotropy energy per unit length of the band (aside from the anisotropy contribution to the energy of the residual Néel wall) is

$$W_{a} = \frac{DK}{2B \tan \Theta} \int_{-B}^{B} dx \int_{-(B+x)\tan\Theta}^{(B+x)\tan\Theta} dy \sin^{2} \phi$$
$$= 4DKB \langle \sin^{2} \phi \rangle, \tag{4}$$

where K is the in-plane uniaxial anisotropy constant and where the average is taken over the band or, equivalently, over one of the triangular regions. For a fanlike configuration and small Θ , one gets

$$\langle \sin^2 \phi \rangle \approx \frac{1}{3} \Theta^2.$$
 (5)

For a Néel wall whose width is much less than the thickness of the film, the energy per unit length of wall [7] is $4\pi DM_s(\pi A)^{1/2}$. With the Gd-Co parameters this is a reasonable estimate since the Néel wall is much smaller than the film thickness. (Under such circumstances, for some materials, e.g., Permalloy, the Bloch wall would be energetically preferred to the Néel wall, but we are assuming that the anisotropy energy associated with M normal to the film is so large that only the Néel wall can occur.) One then has, for the energy per unit length along the horizontal,

$$W_{\rm n} = \frac{1}{\sin \Theta} 4\pi D M_{\rm s} (\pi A)^{1/2} \approx \frac{1}{\Theta} 4\pi D M_{\rm s} (\pi A)^{1/2},$$
 (6)

where in the last equality we have again assumed small Θ .

From Eqs. (3), (4), and (6) we now have for the energy per unit horizontal length

$$W = W_{\rm m} + W_{\rm a} + W_{\rm n}$$

$$= 8M_{\rm s}^2 D^2 \left(3 - 2 \ln \frac{2B}{s} \right) + \frac{4}{3} DKB\Theta^2$$

$$+ \frac{1}{\Theta} 4\pi DM_{\rm s} (\pi A)^{1/2}, \tag{7}$$

which, when minimized with respect to B and Θ , yields

$$\Theta = \frac{\pi (\pi A)^{1/2}}{8M_{s}D},$$

$$B = \left(\frac{768}{\pi^{3}}\right) \frac{M_{s}^{4}D^{3}}{KA}.$$
(8)

The results for three different samples of Gd-Co are shown in Table 1. In all cases it is assumed that the exchange constant is $A = 2.5 \times 10^{-14}$ J/cm $(2.5 \times 10^{7}$ ergs/cm). That the numerical agreement is poor is not surprising, given the approximations of the treatment. A more cogent test of the functional relationships is obtained from an examination of the ratios of Θ and B for three samples, which yield

$$\Theta_{\mathbf{a}} : \Theta_{\mathbf{b}} : \Theta_{\mathbf{c}} = \begin{cases} 1.0 : 1.4 : 0.74, \text{ observed,} \\ 1.0 : 1.5 : 0.63, \text{ calculated;} \end{cases}$$

$$B_{\mathbf{a}} : B_{\mathbf{b}} : B_{\mathbf{c}} = \begin{cases} 1.0 : 0.7 : 1.5, \text{ observed,} \\ 1.0 : 0.16 : 3.3, \text{ calculated.} \end{cases}$$

The ratios for Θ are surprisingly good. The lack of agreement of B suggests that the calculated dependence of B on M_s and on D is too strong.

Ion-implanted layers in garnet films

Whereas the Gd-Co films have an easy in-plane axis of magnetization, the ion-implanted garnet films have trigonal symmetry in the presence of a perpendicular bias field with three easy *directions* of magnetization. This is a consequence of the cubic anisotropy of the garnet. The garnets are grown with a [111]-axis perpendicular to the film. With the polar axis taken as normal to the film and the azimuthal angle measured with respect to the $(1, 1, \bar{2})$ direction in the crystal, the cubic anisotropy is expressed as

$$K_1\left(\frac{1}{4}\sin^4\theta + \frac{3}{4}\cos^4\theta + \frac{\sqrt{2}}{3}\sin^3\theta\cos\theta\cos3\phi\right),\,$$

where K_1 is the cubic anisotropy constant. The angle between M and the plane of the film, the complement of θ , will be denoted by η . In the presence of an in-plane field, η depends on the direction of M, but not very sensitively. We ignore this dependence and treat η as a constant. For small η the effective in-plane anisotropy is

$$-\kappa \cos 3\phi$$
, (9)

where the trigonal anisotropy constant is

$$\kappa = \frac{\sqrt{2}}{3} \eta |K_1|. \tag{10}$$

 $(K_1 \text{ is negative in the case of interest.})$ The material used for Fig. 3 had $M_s \approx 4 \times 10^{-3} \text{ T (40 Gs)}$, a normal uniaxial anisotropy constant K_u of about $1.1 \times 10^{-3} \text{ J/cm}^3$ (1.1 $\times 10^4 \text{ ergs/cm}^3$), and a uniaxial anisotropy induced by the

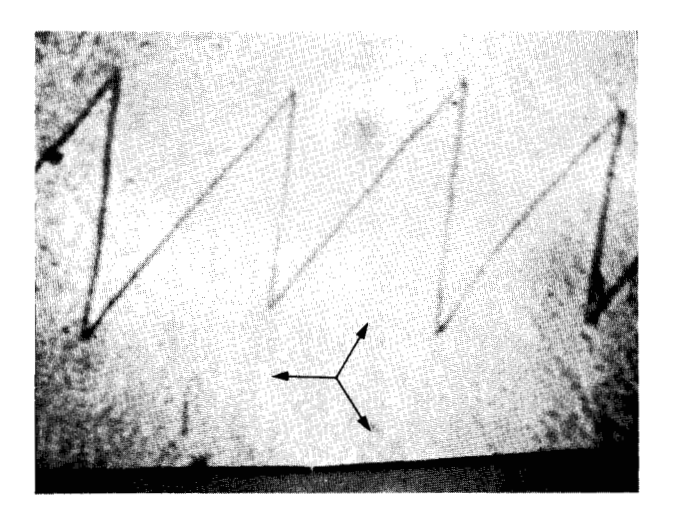


Figure 3 A ferrofluid pattern obtained in an implanted garnet having $M_s = 4 \times 10^{-3}$ T (40 Gs), $\kappa \approx 7.6 \times 10^{-5}$ J/cm³ (7.6 × 10^2 ergs/cm³), and $2D \approx 0.4 \ \mu m$. The arrows indicate the easy magnetization directions.

ion-implantation of -2.6×10^{-3} J/cm³ (-2.6×10^{4} ergs/cm³). The analysis of Lin *et al*. [8] yields $\eta \approx 0.27$. If we take as a rather characteristic value of K_1 for such compositions $K_1 \approx -0.6 \times 10^{-3}$ J/cm³ (-0.6×10^{4} ergs/cm³), we get $\kappa \approx 7.6 \times 10^{-5}$ J/cm³ (7.6×10^{2} ergs/cm³).

We now consider two domains, each having its magnetization along a preferred direction, abutting each other as shown in Fig. 4. For the garnet layer the angle ψ in Fig. 4 is 30°. The charge per unit length along the interface of the domains is $4M_sD\cos\psi$. As before, we calculate the stray field as if the charge were uniformly distributed over the band of width 2B. The maximum deviation of M from a preferred axis is Θ . The anisotropy energy is estimated by using a fanlike configuration for which

$$\langle \phi \rangle = \frac{1}{3} \Theta^2.$$

One then finds that the magnetostatic energy is as in Eq. (3) but is multiplied by $\cos^2 \psi$. (One factor of $\cos \psi$ arises from the charge density, the other from the angle between M and the stray field.) For the anisotropy energy per unit horizontal length one finds

$$W_{\rm a} \approx 18 D_{\kappa} B \langle \phi^2 \rangle = 6 D_{\kappa} \Theta^2. \tag{11}$$

Within the residual Néel wall the magnetization rotates through an angle $(\pi - 2\psi)$. Middlehoek [7] obtains for the approximate energy per unit length of such a wall

$$8DM_{\rm s}(\pi A)^{1/2} \left(\frac{\pi}{2} - \psi\right) (1 - \sin \psi). \tag{12}$$

333

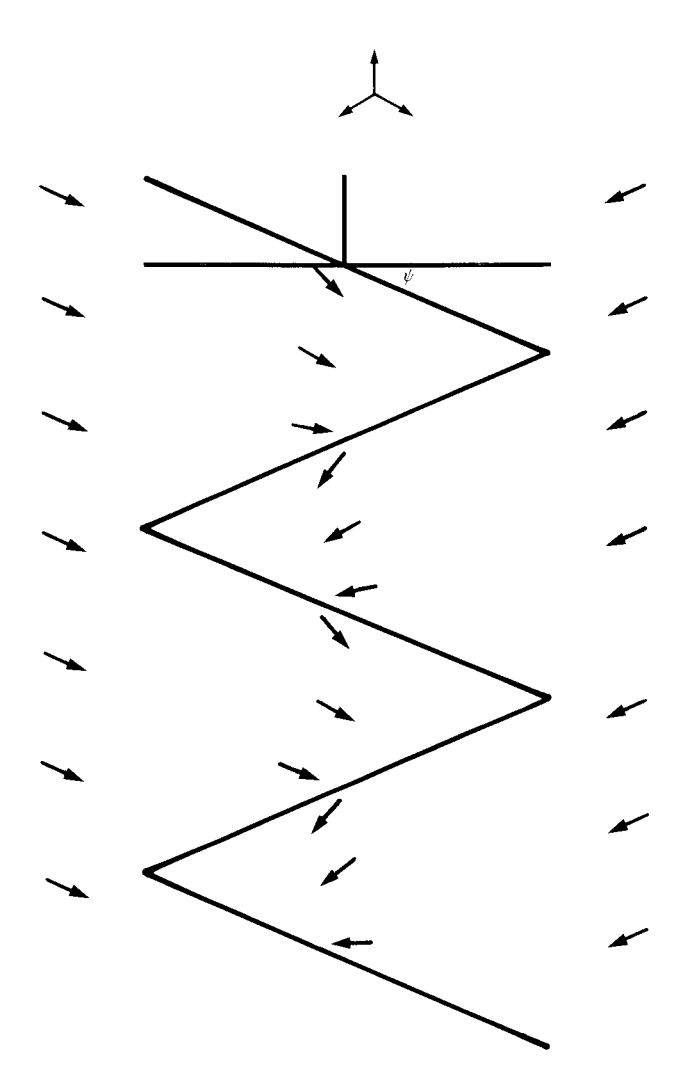


Figure 4 The magnetic configuration assumed for the implanted layer of the garnet. The easy directions of magnetization are indicated on the left.

(We assume that the uniaxial anisotropy induced by the ion implantation is large enough to stabilize the Néel-type wall as compared with a Bloch wall.)

We now have, for the energy per unit length along the horizontal

$$W = 8M_s^2 D^2 \left(3 - 2 \ln \frac{2B}{s} \right) \cos^2 \psi + 6D\kappa B\Theta^2 + \frac{1}{\Theta} 8DM_s (\pi A)^{1/2} \left(\frac{\pi}{2} - 4 \right) (1 - \sin \psi).$$
 (13)

When minimized with respect to Θ and B and with $\psi = \pi/6$, Eq. (13) yields

$$\Theta = \left(\frac{\pi}{18}\right) \left(\frac{(\pi A)^{1/2}}{M_c D}\right),\,$$

$$B = \left(\frac{648}{\pi^3}\right) \left(\frac{M_s^4 D^3}{\kappa A}\right). \tag{14}$$

For the garnet film it is estimated that $M_{\rm s} = 4 \times 10^{-3} \, {\rm T}$ (40 Gs), $D = 0.2 \, \mu{\rm m}$, $\kappa = 0.76 \times 10^{-4} \, {\rm J/cm}^3$ (7.6 $\times 10^2 \, {\rm ergs/cm}^3$), and $A = 2.5 \times 10^{-14} \, {\rm J/cm}$ (2.5 $\times 10^{-7} \, {\rm ergs/cm}$). We then obtain

$$2\Theta = \begin{cases} 34^{\circ}, \text{ observed,} \\ 22^{\circ}, \text{ calculated;} \end{cases}$$

$$2B = \begin{cases} 20 \ \mu\text{m, observed,} \\ 45 \ \mu\text{m, calculated.} \end{cases}$$

The numerical agreement is poor but no worse than one might expect from such an approximate treatment and the uncertainties in the parameters for the implanted layer. The magnitudes are such that it is not unreasonable to anticipate that the functional relationships are correct. One point in particular may be noted that is most readily susceptible to comparison with experiment: A change in the bias field can influence no parameter other than κ . Therefore, while there will be a change in the scale of the zigzag with bias field, the vertex angle will be relatively unaffected.

Closure domains in garnet at a straight edge

The trigonal symmetry of the garnet suggests that at a feature such as a straight-edge boundary between an implanted and unimplanted region, closure domains in the implanted region will generally be bounded by walls that carry a magnetic charge. The following treatment was motivated by the goal of seeing if the simple considerations employed here could be used to predict the form of closure domains. The discussion also touches on the general problem of charged walls at unimplanted features.

We have previously dealt with a symmetrical zigzag wall, in which successive segments of the wall formed the sides of isosceles triangles, and the horizontal axis of the wall made equal angles with the magnetizations of the two domains. As a step towards the consideration of closure domains we first treat an asymmetrical wall in an applied magnetic field as shown in Fig. 5. We shall consider the field to be much smaller than the critical field for the trigonal anisotropy. A horizontal wall bounding these domains would carry a charge per unit length

$$\sigma = -2M_s D(\cos \Phi_0 - \cos \Phi_1). \tag{15}$$

Now consider a zigzag wall that extends horizontally as shown in Fig. 5. The lengths of the wall segments are

$$\ell_1 = \frac{2B}{\sin \theta_1}, \qquad \ell_2 = \frac{2B}{\sin \theta_2}, \tag{16}$$

and the period of the structure is

$$\Lambda = 2B(\cot \theta_1 - \cot \theta_2). \tag{17}$$

The vertex angle of the zigzag is denoted by

$$2\Theta = \theta_2 - \theta_1. \tag{18}$$

The situation, somewhat more general than the symmetric zigzag, can be treated in a similar way by starting from the fundamental presumption: Each segment of a zigzag wall has a direction that deviates by only a small angle from the direction of an uncharged wall that would bound the same two domains. The charge that is associated with this deviation is then distributed over a band containing the wall. Consider the uncharged walls shown in Fig. 6 bounding domains having the same orientations as those in Fig. 5. Within each wall M turns through an angle $(\Phi_0 + \Phi_1)$. Now, with centers of rotation lying along a horizontal line in the figure, rotate the successive walls alternately through the angles ε_1 clockwise and ε_2 counterclockwise, and thereby obtain the zigzag of Fig. 5 with

$$\begin{split} \Theta_1 &= \frac{\Phi_1 - \Phi_0}{2} - \varepsilon_1, \\ \Theta_2 &= \frac{\Phi_1 - \Phi_0}{2} + \varepsilon_2. \end{split} \tag{19}$$

We consider the rotation as carrying along M within the wall and so preserving the uncharged character of the Néel wall, the charge being taken up through deformations in the adjoining medium. Then the residual wall is still a $(\Phi_0 + \Phi_1)$ -wall with its energy per unit length given by Eq. (13) with $[(\pi/2) - \psi]$ replaced by $(\Phi_0 + \Phi_1)/2$. To obtain the energy per unit length along the horizontal one introduces the geometrical factor $(\ell_1 + \ell_2)/\Lambda$. Thus the Néel wall energy per unit horizontal length is, to first order in ε_1 , ε_2 ,

$$\begin{split} &4M_{\rm s}D(\pi A)^{1/2}(\Phi_0+\Phi_1)\left(1-\cos\frac{\Phi_0+\Phi_1}{2}\right)\\ &\times\frac{2\sin\left[(\Phi_1-\Phi_0)/2\right]+(\varepsilon_2-\varepsilon_1)\cos\left[(\Phi_1-\Phi_0)/2\right]}{\varepsilon_1+\varepsilon_2}\,. \end{split}$$

(20)

To estimate the anisotropy and field energy we note that Φ_0 and Φ_1 are such as to minimize the energy density of each of the two domains. For small fields the energy density in the zigzag band is proportional to the square of the deviation of M from $\Phi_0 + \Phi_1$. If the angular deviation of M from the domain orientation is denoted as ϕ , then within the band the average energy density associated with the anisotropy and the applied field is $c_0 \langle \phi^2 \rangle$ and $c_1 \langle \phi^2 \rangle$ in the upper and lower triangular areas, respectively. For small applied fields one finds

$$c_0 = 9D\kappa \left\{ 1 + \frac{HM_s}{9\kappa} \cos \theta \right\},\,$$

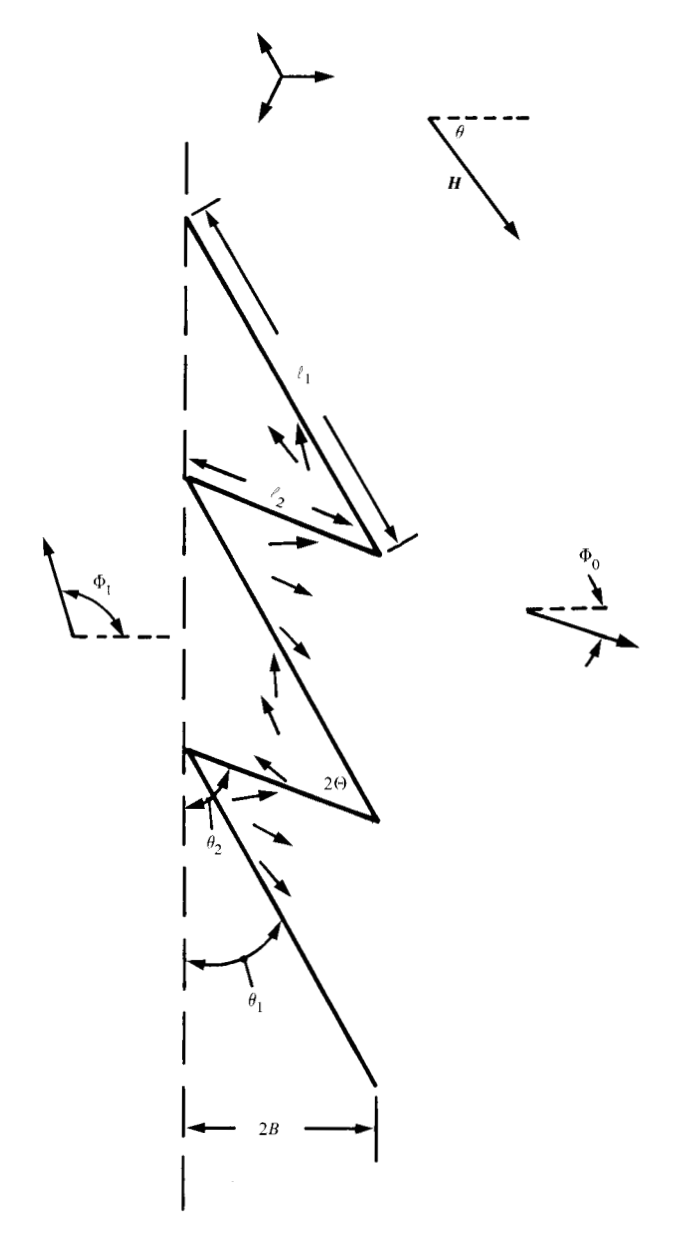


Figure 5 Magnetic configurations assumed for asymmetric wall and for closure domains at an edge. The easy directions of magnetization are indicated on the left. The horizontal dashed line is the edge for this array of closure domains.

$$c_1 = 9D\kappa \left\{ 1 + \frac{HM_s}{9\kappa} \cos\left(\theta + \frac{2\pi}{3}\right) \right\}. \tag{21}$$

The assumption of a fanlike configuration leads to the estimate

$$\langle \phi_2 \rangle = \frac{1}{6} \left(\varepsilon_1^2 + \varepsilon_2^2 \right). \tag{22}$$

The magnetostatic energy is, as before,

$$\sigma^2 \left(\frac{3}{2} + \ln \frac{2}{2B} \right), \tag{23}$$

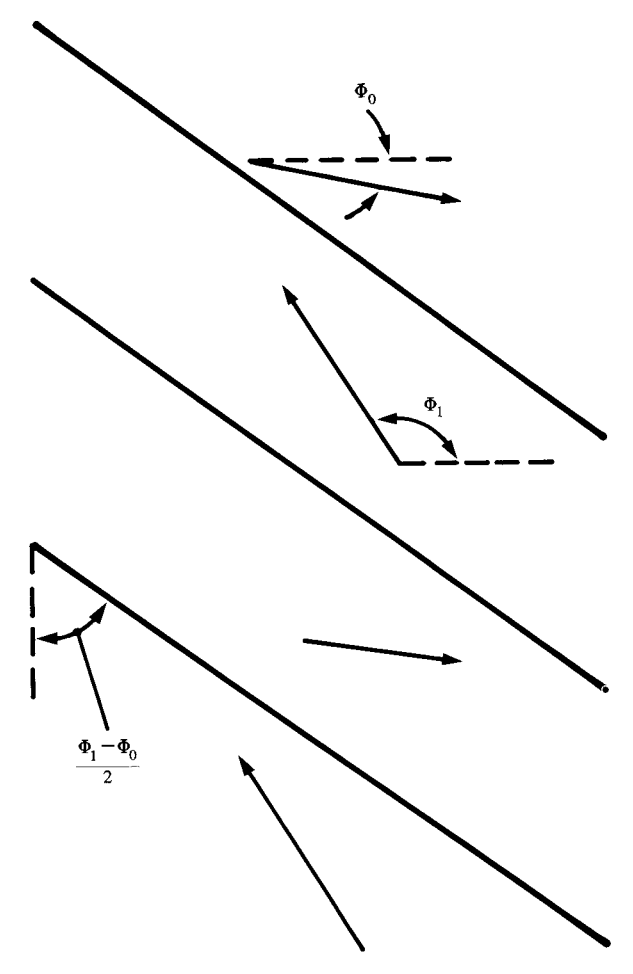


Figure 6 Array of uncharged domain walls from which the wall of Fig. 5 is obtained.

with σ given by Eq. (15). We can now write the estimated total energy in terms of ε_1 , ε_2 , and B, and determine these parameters by minimization of the energy.

To deal with the straight edge we simply cut off the material immediately below the horizontal band along the dashed line in Fig. 5. This introduces an edge along which there is a charge with linear density

$$\sigma_0 = 2M_c D \cos \Phi_1. \tag{24}$$

The magnetostatic energy of interaction between this edge charge and the band of charge is easily calculated as σ_0 times the magnetostatic potential at the edge due to the band. This yields

$$-8M_s^2D^2\cos\Phi_1(\cos\Phi_0-\cos\Phi_1)\left[1+\ln\left(\frac{s}{2B}\right)\right]. \quad (25)$$

We ignore other interactions associated with the edge charge although it is clear that a major modification involves the value of Φ_1 . Thus, we have as our estimation of the energy of the configuration in the presence of the edge,

$$W = 4M_{s}D^{2}(\cos\Phi_{0} - \cos\Phi_{1})^{2}\left(\frac{3}{2}\ln\frac{s}{2B}\right)$$

$$+ 8M_{s}^{2}D^{2}\cos\Phi_{1}(\cos\Phi_{0} - \cos\Phi_{1})\left(1 + \ln\frac{s}{2B}\right)$$

$$+ 4M_{s}D(\pi A)^{1/2}(\Phi_{0} - \Phi_{1})$$

$$\times \left(1 - \cos\frac{\Phi_{0} + \Phi_{1}}{2}\right)\sin\frac{\Phi_{1} - \Phi_{0}}{2}.$$
 (26)

Ignoring the term that is independent of ε_1 , ε_2 , and B, we write this as

$$W = P \ln \frac{s}{2B} + 2 \frac{2 \sin \left[(\Phi_1 - \Phi_0)/2 \right] + (\varepsilon_2 - \varepsilon_1) \cos \left[(\Phi_1 - \Phi_0)/2 \right]}{\varepsilon_1 + \varepsilon_2} + RB(\varepsilon_1^2 + \varepsilon_0^2), \tag{27}$$

in which we have omitted a constant term, and where

$$P = 4M_{\rm s}^2 D^2 (\cos^2 \Phi_0 - \cos^2 \Phi_1),$$

$$Q = 4M_{\rm s}D(\pi A)^{1/2}(\Phi_0 + \Phi_1)\left(1 - \cos\frac{\Phi_0 + \Phi_1}{2}\right),$$

and

$$R = 3D\kappa \left[1 + \frac{HM_s}{18K} \cos\left(\theta + \frac{\pi}{3}\right) \right]. \tag{28}$$

Minimization with respect to ε_1 , ε_2 , and B leads to equations that can be easily solved;

$$\varepsilon_{1} = \frac{Q}{P} \left\{ 1 + \sqrt{\frac{P - Q \cos \left[(\Phi_{1} - \Phi_{0})/2 \right]}{P + Q \cos \left[(\Phi_{1} - \Phi_{0})/2 \right]}} \right\}^{-1} \sin \frac{\Phi_{1} - \Phi_{0}}{2},$$

$$\varepsilon_{2} = \frac{Q}{P} \left\{ 1 + \sqrt{\frac{P + Q \cos \left[(\Phi_{1} - \Phi_{0})/2 \right]}{P - Q \cos \left[(\Phi_{1} - \Phi_{0})/2 \right]}} \right\}^{-1} \sin \frac{\Phi_{1} - \Phi_{0}}{2},$$

and

$$B = \frac{P^2}{RQ^2} \left(\frac{P + \{P^2 - Q^2 \cos^2[(\Phi_1 - \Phi_0)/2]\}^{1/2}}{\sin^2[(\Phi_1 - \Phi_0)/2]} \right). \tag{29}$$

Evidence that closure domains of the form that we have envisioned do exist is found in some of the ferrofluid pictures taken by S. Schwarzl [9]. Figure 7(a, b) shows two such photographs from Schwarzl's work. The orientation of the edge is at about 15° with an easy direction of magnetization, rather than at right angles to one of the easy directions (as assumed above). With the angles Φ_0 and Φ_1 defined as in Fig. 8, Eqs. (28) and (29) still hold, and for

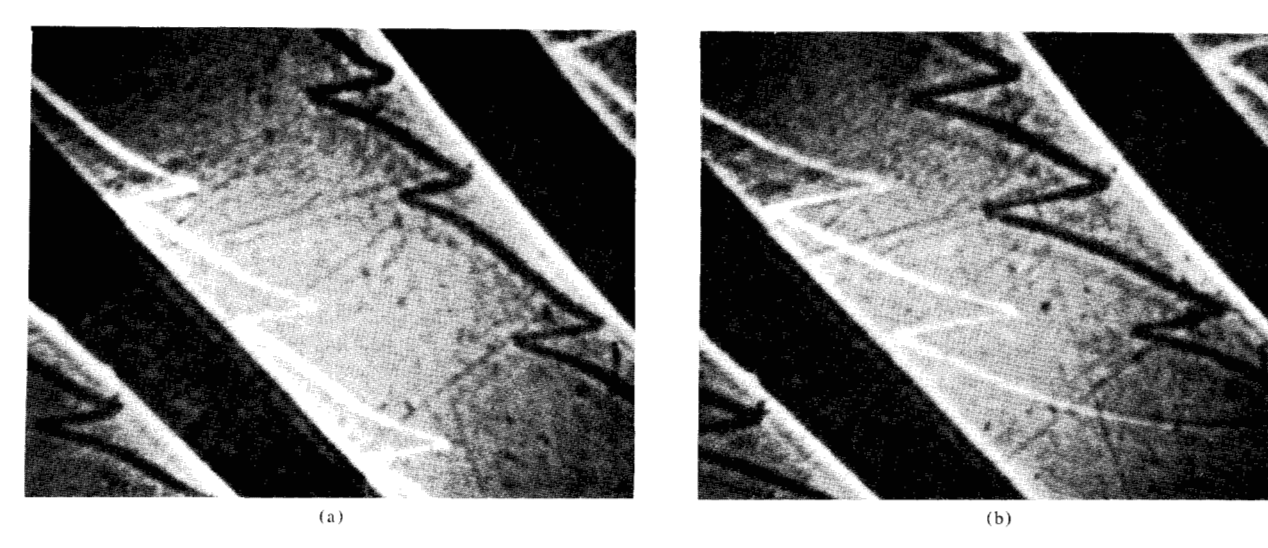


Figure 7 Ferrofluid pattern of closure domains at the straight-edge boundary of implanted layer of garnet having $4\pi M_s = 0.1097$ T (1097 Gs), $\kappa \approx 9 \times 10^{-5}$ J/cm³ (9.0 × 10² ergs/cm³), and $2D \approx 4800$ μ m. The heavy bars (unimplanted regions) are 15 μ m wide. (a) $2B \approx 10$ μ m; $2\Theta = 46^{\circ}$; (b) $2B \approx 15$ μ m; $2\Theta = 36^{\circ}$.

H=0 one has $\Phi_0=\pi/12$ and $\Phi_1=7\pi/12$. For Schwarzl's sample the available data indicate that $4\pi M_s=0.1097$ T (1097 Gs), $2D=0.48~\mu m$, $A=2.5\times10^{-14}$ J/cm (2.5 \times 10^{-7} ergs/cm), and $\kappa=9\times10^{-5}$ J/cm³ (900 ergs/cm³). With these values Eqs. (21) and (31) yield $\theta_1=33^\circ$, $\theta_2=53^\circ$, $2\Theta=21^\circ$, and $2B=68~\mu m$. For comparison, the heavy bar in the figure is approximately $15~\mu m$ wide. For Fig. 7(a) one gets approximately $2B=10~\mu m$ and $2\Theta=46^\circ$; for Fig. 7(b) one obtains from the photograph $2B=15~\mu m$ and $2\Theta=36^\circ$. The numerical agreement is not very good, as one might expect. What is more interesting is the period of the structure that can be obtained from Eq. (17), yielding $\Lambda=23~\mu m$. In the photographs there is some variation in the periods, but in each photograph, for the structure that is seen, the average period is $23~\mu m$.

It seems clear that the amplitude of the zigzag boundary of the closure domains is quite sensitive to the direction of the magnetic field, whereas in our treatment the dependence of the amplitude on H is through $HM_{\rm s}/18\kappa\approx 0.03$ for the parameters of Schwarzl's sample. It may be that as the field was rotated in Schwarzl's series of photographs the configuration of closure domains was becoming unstable relative to a continuously curling configuration. There is evidence for this in Fig. 7(b). There is also the effect of interactions of the two bars lying close to each other in the area photographed. Another point is that at some time during the experiment, for some orientation of the magnetic field, these closure domains were established with some amplitude, vertex angle and period. The zigzag wall was presumably anchored at the ends of the

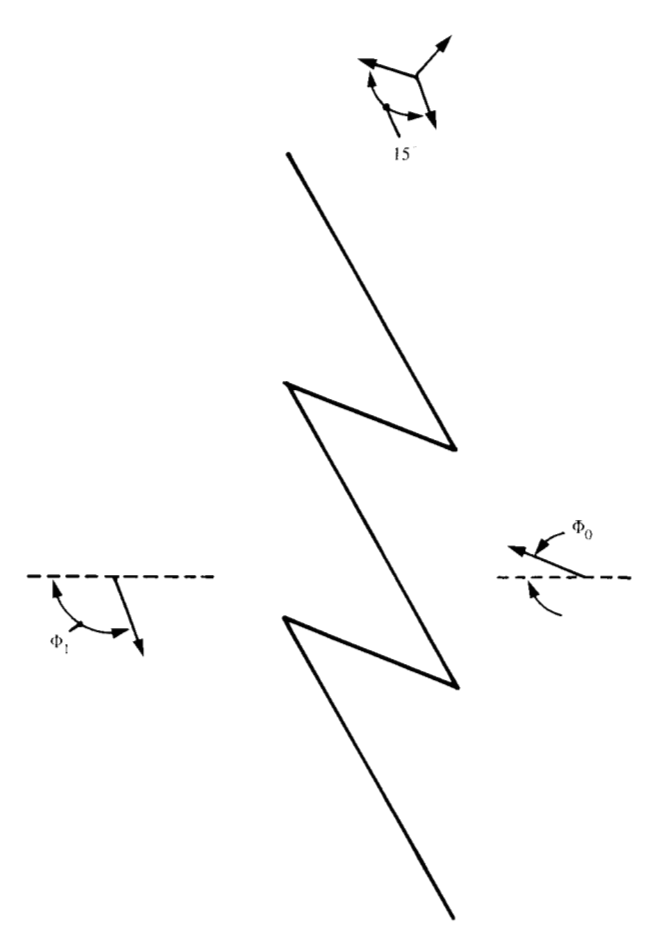


Figure 8 Definition of Φ_0 , Φ_1 for the positive (dark) charged walls in Fig. 7.

337

bar, which unfortunately are not shown in the photograph. The number of closure domains was fixed at that time since there is no continuous way to change that number as the field is rotated. Thus, the closure domains seen in Fig. 7(a, b) need not be equilibrium configurations but may be constrained to have the same average period as the presumed equilibrium configurations when the domains were first established.

It is somewhat reassuring that the predicted shape of the closure domains is correct, and that the predicted amplitude, angle, and particularly the period, are reasonable. This suggests that the functional dependences are reliable and that the approximate considerations used here can be useful in related problems.

Summary

The static charged walls in Gd-Co films and in the ionimplanted layer of garnet materials have been examined theoretically with allowance made in an exaggerated way for the spread of magnetic charge into a wider region than the thin wall seen in the ferrofluids pictures. One finds that both the vertex angle and the zigzag amplitude, that is, the scale of the structure, are determined by intrinsic properties of the films. These considerations lead to a prediction of the form of closure domains bounded by charged walls arising at straight edges in the ion-implanted garnet. The prediction is found to be qualitatively correct.

Acknowledgment

I am grateful to A. Malozemoff for calling my attention to the unusual wall in a film of Gd-Co, to J. Slonczewski for his perceptive criticism and comments, and to D. Dove and S. Schwarzl for their pictures of kinked charged walls.

References and notes

- 1. J. P. Jakubovics, Phil. Mag. 30, 111 (1974).
- (a) R. C. Taylor and A. Gangulee, J. Appl. Phys. 47, 4666 (1976). The films were evaporated from a double e-beam source with the substrate at ambient temperature. The film was approximately 0.5 μm thick. (b) Private communication with S. Schwarzl and R. C. Taylor, IBM Research Division, Thomas J. Watson Research Center, Yorktown Heights, NY 10598
- 3. The Permalloy used in these experiments was fabricated in our laboratories.
- our laboratories.
 4. E. J. Hsieh and R. F. Soohoo, AIP Conf. Proc. 5, 727 (1971).
- 5. D. D. Dressler and J. H. Judy, IEEE Trans. Magnetics 10, 674 (1974).
- 6. N. Minnaja and M. Nobile, AIP Conf. Proc. 10, 1001 (1972).
- S. Middlehoek, "Ferromagnetic Domains in Thin Ni-Fe Films," Van Soest, Amsterdam, 1961.
- Y. S. Lin, G. S. Almasi, and G. E. Keefe, *IEEE Trans. Magnetics* 13, 1744 (1977).
- S. Schwarzl and Y. S. Lin, IBM Research Division, Thomas J. Watson Research Center, Yorktown Heights, NY 10598, private communication.

Received November 1, 1978; revised December 1, 1978

The author is a staff member at the IBM Thomas J. Watson Research Center, Yorktown Heights, New York 10598, but is currently on faculty loan to Spelman College, Mathematics Dept., Spelman Lane, Atlanta, Georgia 30314.